Gene expression-signature of belinostat in cell lines is specific for histone deacetylase inhibitor treatment, with a corresponding signature in xenografts

Anne Monks[a], Curtis D. Hose[a], Patrick Pezzoli[c], Sudhir Kondapaka[b], Gordon Vansant[c], Kamille Dumong Petersen[d], Maxwell Sehested[d], Joseph Monforte[c] and Robert H. Shoemaker[b]

Belinostat is a hydroxamate-type histone deactylase inhibitor (HDACi), which has recently entered phase I and II clinical trials. Microarray-based analysis of belinostat-treated cell lines showed an impact on genes associated with the G_2/M phase of the cell cycle and downregulation of the aurora kinase pathway. Expression of 25 dysregulated genes was measured in eight differentially sensitive cell lines using a novel high-throughput assay that combines multiplex reverse transcriptase-PCR and fluorescence capillary electrophoresis. Sensitivity to belinostat and the magnitude of changes in overall gene modulation were significantly correlated. A belinostat-gene profile was specific for HDACi in three cell lines when compared with equipotent concentrations of four mechanistically different chemotherapeutic agents: 5-fluorouracil, cisplatin, paclitaxel, and thiotepa. Belinostat- and trichostatin A (HDACi)-induced gene responses were highly correlated with each other, but not with the limited changes in response to the other non-HDACi agents. Moreover, belinostat treatment of mice bearing human xenografts showed that the preponderance of selected genes were also modulated *in vivo*, more extensively in a drug-sensitive tumor than a more resistant model. We have demonstrated a gene signature that is selectively regulated by HDACi when compared with other clinical agents allowing us to distinguish HDACi responses from those related to other mechanisms. *Anti-Cancer Drugs* 20:682–692 © 2009 Wolters Kluwer Health | Lippincott Williams & Wilkins.

Anti-Cancer Drugs 2009, **20**:682–692

Keywords: belinostat, gene signature, histone deacetylase inhibitor

[a]STB Laboratory of Functional Genomics, SAIC-Frederick Inc., [b]Screening Technologies Branch, DTP, NCI-Frederick, Frederick, Maryland, [c]Althea Technologies Inc., Express Pathway and Biomarker Group, San Diego, California, USA and [d]TopoTarget A/S, and Rigshospitalet, Copenhagen, Denmark

Correspondence to Dr Anne Monks, PhD, SAIC-Frederick Inc., PO Box B, NCI-Frederick, 1032 Boyles Street, Frederick, MD 21702, USA
Tel: +1 301 846 5528; fax: +1 301 846 6081;
e-mail: monksa@mail.nih.gov

Received 18 March 2009 **Revised form accepted** 13 May 2009

Introduction

Chromatin remodeling is regulated in part through the opposing activities of histone acetyl transferases and histone deactylases (HDACs) [1]. Acetylation of their histone tails leads to open and closed forms of chromatin, which alters accessibility of transcription factors to DNA [2]. Inhibitors of HDAC (HDACi), which are being developed as potential anticancer agents [3,4], cause accumulation of acetylated proteins, particularly histones, alter chromatin structure leading to a change in gene transcription, and induce apoptosis [5,6].

Gene expression changes have been evaluated in response to a variety of inhibitors of HDAC [7–9], and up to *22%* of genes were identified as showing expression changes in response to HDACi treatment [9]. These were diverse genes impacting multiple pathways important for cell survival and proliferation. Cell cycle analysis indicates that HDACi may impact two distinct checkpoints [10], inhibiting cells at the G_1/S, mainly by inducing expression of the cyclin-dependent kinase inhibitor p21/CIP1/WAF1 [11] and G_2/M by downregulation of cyclin B1 [12]. Moreover, as a growing number of nonhistone, acetylated targets of HDACi are identified [13], it becomes more likely that modulation of these proteins may contribute to drug-induced cell death. Thus, there may be multiple mechanisms underlying the activity of HDACi, possibly related to the specificity of the HDAC class targeted by the agent, but this remains an open question [4]. However, due to the diverse cellular response to inhibitors of HDAC, which can be different in different tumor models, HDACi may represent a class of agents that do not generate rapid resistance owing to their effect on a range of cellular processes.

Belinostat (PXD101, NSC 726630) is a hydroxamate-class HDACi with in-vitro activity against a variety of human cell lines and in-vivo activity against ovarian, colon, and bladder xenografts [14–16]. Belinostat has been shown to inhibit both class I and II HDAC isoforms with similar efficacy [17], and exhibits synergistic toxicity in combination with 5-fluorouracil [18] and bortezimib [19],

0959-4973 © 2009 Wolters Kluwer Health | Lippincott Williams & Wilkins DOI: 10.1097/CAD.0b013e32832e14e1

carboplatins, and taxanes [15]. To date, more than 500 patients have been treated with belinostat in a number of phase I and II clinical trials. A report from a phase I trial in patients with advanced solid tumors indicated that the drug is well tolerated with a terminal half life of approximately 1 h, and a C_{max} (maximum plasma concentration) of approximately 32 μg/ml at the recommended phase II dose [20]. In a study to evaluate biomarkers for this agent in multiple cell lines, sensitivity to belinostat was correlated with basal expression of several genes, but not with acetylation of either histone or tubulin [21], although in A2780 xenografts, the level of H4 acetylation was related to plasma and tumor pharmacokinetics [22].

Here, we report a gene profile for HDACi across a variety of cell lines which is specific to HDACi compared with four other antineoplastic agents of different mechanisms. These data were associated with the G_2/M phase of the cell cycle and led us to determine an indirect effect on expression of aurora kinase A and B proteins. Moreover, *in vivo*, this selected subset of genes was largely dysregulated in a belinostat-sensitive tumor, A2780, but to a lesser extent in the more resistant PC-3 tumor. The fact that most of these changes are consistent across otherwise heterogeneous tumor cell lines and that they occur not only in cell culture, but also in xenograft models, suggests they may provide a mechanism to assess in-vivo response in tumors or surrogate markers.

Methods

Cell lines and reagents

Cell lines were utilized from the NCI-60 cell line screen, grown in RPMI-1640 (Lonza, Walkersville, Maryland, USA), 5 μmol/l L-glutamine, and 5% fetal bovine serum. Belinostat was provided by TopoTarget (Copenhagen, Denmark), trichostatin A (TSA) was purchased from Sigma (St. Louis, Missouri, USA) and all other agents were provided by the Drug Synthesis and Chemistry Branch of the Developmental Therapeutics Program, National Cancer Institute (NCI).

Xenografts

Female NMRI mice, 6–8 weeks old, were obtained from Charles River Laboratories, Germany. The experiment was conducted at TopoTarget, Copenhagen, and approved by the Experimental Animal Inspectorate, Danish Ministry of Justice. All animals were housed and maintained under high hygiene standard conditions and provided with standard food and water *ad libitum*. Mice were acclimatized for at least a week and then injected subcutaneously with 1e7 A2780 human ovarian carcinoma (a gift from R. Ozols, Fox Chase Cancer Centre, Philadelphia, Pennsylvania, USA) or PC-3 (CRL-1435) human prostate cancer cells. The cells were grown in RPMI + 10% fetal bovine serum, washed once with PBS and suspended in 100 μl of PBS, and then suspended in 100 μl matrigel (Becton Dickinson and Company, Franklin Lakes, New Jersey, USA) before injection. Tumor diameters were measured during tumor growth and tumor volumes estimated according to the formula: (width^2 × length)/2. When tumor size reached 600 ± 150 mm^3 (A2780) or 750 ± 200 mm^3 (PC-3), mice were randomized into treatment groups and treatment initiated. Belinostat was used in the clinical formulation in L-arginine/isotonic sterile saline (pH approximately 9.4) and injected 200 mg/kg 100 μl/10 g in the tail vein at $t = 0$, 1.5, and 3 h. At $t = 6$ and 24 h after first dose, groups of three mice were sacrificed. Vital tumor fragments (100–200 mg) were immersed in RNAlater stabilization reagent (1 ml per tumor sample; Qiagen, Valencia, California, USA). The tumor fragments were minced slightly to ensure full solution penetration and stored at −20°C until analysis.

Microarray

Human OncoChip (35K cDNA arrays from the NCI/Center for Cancer Research microarray center) were utilized according to published protocols on the mAdB homepage (*www.nicarray.nci.nih.gov*).

Total RNA was extracted from cell lines treated with belinostat and TSA for 6 and 24 h, plus control, untreated cell lines at the same time points, then reverse transcribed and amino-allyl modified dUTP was incorporated (Labelstar kit, Qiagen), then chemically coupled to a Cy3 or Cy5 fluorescently labeled dye. The appropriate treated versus control RNA was combined and hybridized to arrays at 42°C for 16 h. Fluorescence was read on a GenePix 4100A microarray scanner and data was analyzed through GenePix Pro 4.1 software (Molecular Devices, Sunnyvale, California, USA), and then the files were uploaded to the NCI/Center for Cancer Research microarray centers mAdB gateway, where they were analyzed with available tools including significance analysis of microarrays [23], prediction analysis of microarrays [24], and DAVID/EASE functional analysis [25].

Quantitative real time reverse transcriptase-PCR

Reactions were measured using the ABI prism 7700 Sequence Detection System and TaqMan Chemistries (Applied Biosystems, Foster City, California, USA). PCR reactions using 5 ng of cDNA were carried out using the TaqMan SYBR green master mix (Applied Biosystems) in 25 μl reactions. Triplicate samples were analyzed using the comparative Ct method (ABI user bulletin #2) and expressed as an increase or decrease in relative expression (log_2) compared with the untreated control.

Multiplexed reverse transcriptase-PCR (XP-PCR)

Chimeric primer pairs were designed for each selected gene with a gene-specific sequence and a universal

sequence common to all forward and reverse primers. Twenty-five nanograms of total RNA was used as template for the reverse transcription reactions. Half of these reactions were carried over as templates for the PCR reactions. A pair of universal primers that recognized the universal sequences in the chimeric primers were included (in excess) in the PCR reaction, with one fluorescently labeled. After a few initial rounds of PCR, the universal primers primarily drive the reactions. The chimeric primers were designed to produce PCR products with an approximately 5 base pair difference between them, resulting in a stratified set of labeled PCR products. The fluorescently labeled PCR reactions were then analyzed by capillary electrophoresis on a Beckman GeXP Genetic Analysis System (Beckman Coulter Inc., Fullerton, California, USA). Gene expression data are given as the ratio of a target gene normalized by a control gene from the same reaction. Heatmaps of the average gene expression data ($\log_2$) was generated using cluster and Treeview software (Eisen Lab, University of California Berkeley, Berkeley, California, USA) [26].

Western blots

Protein (50 μg) from drug treated or control cells was separated by electrophoresis (4–20% Tris–glycine gel), transferred to polyvinylidene fluoride membranes (Invitrogen, Carlsbad, California, USA) and probed with primary (AURKA and AURKB-Cell Signaling, Danvers, Massachusetts, USA) and appropriate secondary antibodies, then developed using enhanced chemiluminescence, and band intensities measured.

Flow cytometry

Approximately 5×10^6 cells were treated with the HDACi for the indicated times, then harvested and fixed with 70% EtOH. Pellets were resuspended in RNase A (0.2 mg/ml) and stained with propidium iodide (0.05 mg/ml) and read using the Becton Dickinson FACScan flow cytometer (Becton Dickinson). Data were analyzed through Modfit LT v. 2.0 (Becton Dickinson) for MAC.

Aurora kinase assays

The enzymes aurora A and B were obtained from Upstate Biotechnology (Uppsala, New York, USA) and biotinylated substrate (polo-like kinase) is obtained from Cell Signaling Technology (Danvers, Massachusetts, USA). The drugs were diluted in kinase buffer to obtain 100, 10, 1 and 0.1 μmol/l concentrations in a final volume of 10 μl. Five microliter of aurora A or B (1 ng/μl) was pretreated with drug for 30 min, and then 5 μl of substrate (1.5 μmol/l) was added. An ATP concentration of 100 μmol/l was maintained in all kinase reactions. After 30 min of incubation, 5 μl of detection mixture of antibody (phospho-polo-like kinase)-conjugated acceptor and streptavidin-conjugated donor beads (Perkin Elmer Life and Analytical Sciences, Waltham, Massachusetts, USA) was added and then incubated for a further hour. Assays were performed in 384-well white plates in a final volume of 20 μl. All the reactions were performed at room temperature. The plates were read on a Fusion-alpha microplate analyzer (Perkin Elmer Life and Analytical Sciences) to measure fluorescence. The data presented is an average of three different experiments.

Results

Microarray expression profile

HCT-116 (colon) was selected for expression profiling and treated in duplicate experiments with 1 μmol/l belinostat for 6 and 24 h, with more robust, but similar changes observed after 24 h. When all the gene expression profiles were queried for the most significantly dysregulated genes (using significance analysis of microarrays at an false discovery rate of 0.06, and delta = 1.5), there were 238 genes selected of which 77% were downregulated while the remaining were upregulated. The DAVID/EASE program was used to categorize the selected gene set [25], and the gene ontology-based functional analysis is shown in Fig. 1. In line with the functional analysis indicating perturbation of genes involved in the cell cycle, particularly mitosis, we confirmed by real time reverse transcription-PCR, the decreased expression of two genes, RAN and TD60 reported to be upstream in the aurora kinase pathway [27,28], and while there was a modest downregulation of both aurora kinase A and B genes (but not C) which did not meet the stringency criteria for gene modulation, we did confirm the downregulation of aurora kinase protein which has recently been reported for HDACi [29].

Effect of belinostat on cell cycle

Figure 2a summarizes the change in distribution of cells within the cell cycle in response to 0.5–2 μmol/l belinostat over 24 h. All cell lines showed an increase in cells in the G_2 phase, accompanied by a loss of cells in the G_1 or S phase of some cell lines indicating a decrease in cells actively replicating their DNA, consistent with the decrease of multiple minichromosome maintenance genes (involved in the initiation of eukaryotic genome replication) seen on the arrays.

Figure 2b shows the effect of 100 nmol/l belinostat on the expression of the aurora kinase A and B proteins. Although there was a limited impact on these proteins after 6 h incubation, there was a significant decrease in all the cell lines except OVCAR-3 after 24 h but as shown in Fig. 2c, belinostat had no direct effect on the phosphorylating activity of aurora kinase A or B.

A novel multiplexed reverse transcriptase-PCR (XP-PCR) assessment of the effect of 0.5–2 μmol/l belinostat on array-selected genes in multiple cell lines

Figure 3 shows the measurement of 25 array-selected genes (identified in Table 1) in seven cell lines after 1, 2, 4, 8, and 24 h incubation with 0.5–2 μmol/l belinostat

Fig. 1

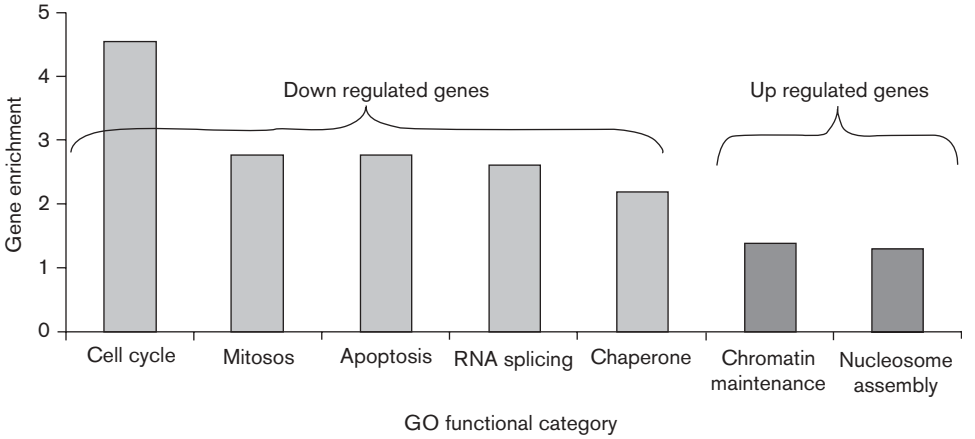

Functional groupings of genes dysregulated in transcriptional profiling studies. Two hundred and thirty-eight genes were found to be significantly dysregulated (SAM analysis with a false discovery rate = 0.06 and a delta = 1.5) in HCT-116 cells treated with belinostat (1 μmol/l). These genes were analyzed by the DAVID gene function classification tool (*http://david.abcc.ncifcrf.gov*), which uses a novel agglomeration algorithm to condense a list of genes and provide a gene enrichment analysis to highlight the most relevant, significant gene ontology (GO) terms associated with this list.

Fig. 2

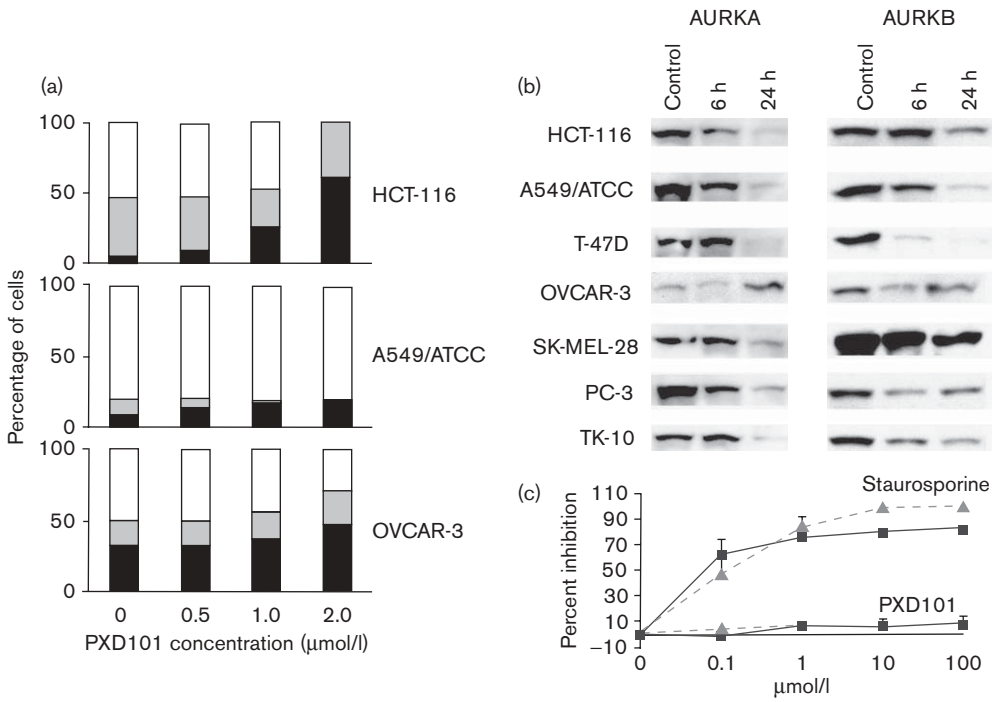

Effects of belinostat on cell cycle distribution and aurora kinase inhibition. (a) Distribution of cells in the cell cycle after treatment with 0.5, 1.0, and 2.0 μmol/l belinostat. Bars represent the percentage of cells in each part of the cell cycle; □ G_1–G_0, ▒ S, G_2–M ■. (b) Western blots of Aurora A (AURKA) and Aurora B (AURKB) protein expression after treatment with 1 μmol/l belinostat for 6 and 24 h in seven human tumor cell lines. (c) Lack of direct inhibition of aurora kinase A (■) and B (□) phosphorylating activity by belinostat compared with staurosporine as a positive control. Data reflect average (+SD) of three independent experiments.

(3A = downregulated genes, 3B = upregulated genes, and 3C = control genes). The aim was to confirm gene expression changes from the arrays in more cell lines and explore how quickly these expression changes occurred after treatment. The multiplex assay allowed for rapid analysis of the 1000 samples generated (each in

Fig. 3

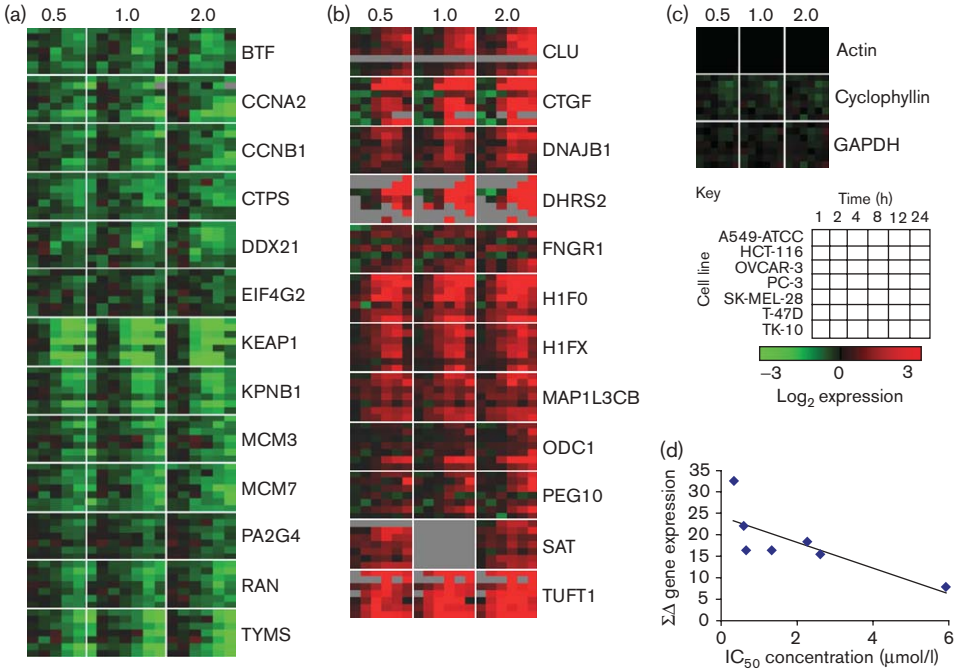

Confirmation of gene expression changes found on microarrays using a novel reverse transcriptase-PCR multiplexed assay-XP-PCR. Eight cell lines were inoculated onto 96 well plates and treated with 0.5, 1.0, and 2.0 μmol/l belinostat and total RNA was collected at 0, 1, 4, 8, 12, and 24 h after drug addition (triplicate wells for each cell line, time, and dose). RNA was then reverse transcribed and gene expression changes for the 1000 samples were measured utilizing the XP-PCR multiplex assay. Gene expression changes compared to the 0 h control samples were calculated (log_2) after normalization to actin and represented as a heatmap where green indicates downregulation, red indicates induction, black shows no change, and grey is missing data. Each block in the heatmap represents the gene expression data for each gene/dose combination where the seven rows are each of the cell lines and the six columns are the belinostat exposure times (as outlined in the key). These data indicate that all eight cell lines have a similar gene response profile to belinostat. IC_{50}, concentration of drug that inhibits 50% of the cell growth. (a) downregulated genes, (b) induced genes, (c) housekeeping genes, (d) identifies the relationship between the sum of the 0.5 μmol/l drug induced changes in genes identified in (a), (b), and (c) after 24 h (sum of the gene expression changes) and the IC_{50} of belinostat for each cell line. This data indicates that the more sensitive the cell line is to belinostat, the greater the magnitude of gene modulation.

triplicate wells), and the relative expression values are plotted as a heatmap [26] to rapidly allow for visual comparisons. The sum of the delta for these genes in each cell line was calculated for the lowest tested concentration (0.5 μmol/l) as a measure of drug-induced gene modulation after 24 h incubation and was found to be negatively correlated to belinostat sensitivity, in these seven cell lines (Fig. 3d), with a Pearson correlation coefficient (PCC) $r = 0.77$ ($P = 0.04$). This indicated that the greater the sensitivity of the cell line to belinostat, the greater the total modulation of the selected genes. There was surprisingly little difference in drug-induced gene perturbations between the selected concentrations, but it was clear that the shorter incubation times (1–4 h) resulted in less modulation of the selected genes than the longer incubations (8–24 h), with the greatest overall change occurring after 24 h.

Specificity of selected gene response for belinostat compared with other antineoplastic agents

Three cell lines, HCT-116 (belinostat sensitive and gene responsive), OVCAR-3 (relatively resistant, but moderately gene responsive), and PC-3 (moderately sensitive but modestly gene responsive) were selected for comparison of gene signatures between belinostat and TSA, another HDACi and a group of four additional antineoplastic drugs. Each cell line was exposed to equipotent concentrations of each of the drugs (belinostat, 0.1 μmol/l; TSA, 0.5 μmol/l; 5-fluorouracil, 20 μmol/l; cisplatin, 10 μmol/l; paclitaxel, 0.025 μmol/l; and thiotepa, 10 μmol/l), resulting in approximately 50% growth inhibition (Fig. 4). Triplicate wells were used for untreated controls and those treated with drugs for 2, 4, 8, and 24 h, in three separate experiments. Each experiment was independently analysed for expression of four control genes and a set of 30 selected genes (Table 1) that had a robust response to belinostat (Table 1 in bold type), and additional related genes functionally involved in belinostat transcriptional response including modulation of the cell cycle, particularly mitosis and the aurora kinase pathway.

Data from these replicate experiments were well reproduced and PCC ranged from 0.71 to 0.80. Figure 5

Table 1 Selected belinostat-associated genes measured by multiplex reverse transcriptase-PCR

Gene	Description	Accession
ABL1*	v-abl Abelson murine viral oncogene homolog 1	NM_005157
AURKA	Aurora kinase A	NM_198436
AURKB	Aurora kinase B	NM_004217
BIRC5	Survivin	NM_001168
BTF	Bcl-2-associated transcription factor	NM_014739
CAD*	Carbamoyl-phosphate synthetase 2	NM_004341
CCNA2	Cyclin A2	NM_001237
CCNB1	Cyclin B1	NM_031966
CDC2	Cell division cycle 2, G_1–S	NM_001786
CDC25B	Cell division cycle 25B	NM_004358
CDK4	Cyclin-dependent kinase 4	NM_000075
CDKN1A	Cyclin-dependent kinase inhibitor 1A (p21)	NM_000389
CDKN2A	Cyclin-dependent kinase inhibitor 2A (p16)	NM_000077
CLU	Clusterin (complement lysis inhibitor)	NM_001831
CTGF*	Connective tissue growth factor	NM_001901
CTPS*	CTP synthase	NM_001905
DDX21	DEAD (Asp-Glu-Ala-Asp) box polypeptide 21	NM_004728
DHRS2*	Short-chain dehydrogenases/reductase family	NM_005794
DNAJB1*	DnaJ (Hsp40) homolog, subfamily B	NM_006145
EIF4G2*	Eukaryotic translation initiation factor 4 gamma, 2	NM_001418
H1FX	H1 histone family, member X	NM_006026
H1F0*	H1 histone family, member 0	NM_005318
IFNGR1	Interferon gamma receptor 1	NM_000416
INCENP	Inner centromere protein	NM_020238
KEAP1	Kelch-like ECH-associated protein 1	NM_012289
KPNB1*	Karyopherin (importin) beta 1	NM_002265
MAP1LC3B*	Microtubule-associated protein 1 light chain 3 β	NM_022818
MCM3	MCM3 minichromosome maintenance deficient 3	NM_002388
MCM7	MCM7 minichromosome maintenance deficient 7	NM_005916
ODC1*	Ornithine decarboxylase 1	NM_002539
PA2G4	Proliferation-associated 2G4, 38 kDa	NM_006191
PEG10	Paternally expressed 10	NM_015068
RAC1	RAS-related C3 botulinum toxin substrate 1	NM_006908
RAN*	RAS-related oncogene family	NM_006325
SAT*	Spermidine/spermine N^1-acetyltransferase	NM_002970
TACC1*	Transforming, acidic coil containing protein 1	NM_006283
TD-60*	Regulator of chromosome condensation 2	NM_018715
TP53*	Tumor protein p53	NM_000546
TUFT1	Tuftelin 1	NM_020127
TPX2	Microtubule-associated, homolog	NM_012112
TYMS*	Thymidylate synthetase	NM_001071

Genes identified with '*' are those representing the specific set of histone deactylase inhibitor-regulated genes. Genes identified by 'italics' are those that were measured in the initial experiments with eight cell lines and shown in Fig. 3, but were replaced in focused set of genes selected for comparison between drugs (Fig. 5). Genes shown in 'bold' were evaluated in both experimental undertakings.

shows a heatmap representing the relative change in expression of these genes in response to treatment with each of the different agents. Using a Student's *t*-test (two-tail), comparing the average response of the two HDACi, relative to the four other neoplastic agents, for each gene and time point, there were no significant differences in any gene modulation patterns after 1 h reflecting the lack of gene expression change in any cell lines after this early time point. After 4 h drug incubation, nine genes were significantly ($P < 0.01$) differentially modulated either up or down by HDACi treatment compared with the other agents. However, with minor exceptions, after 8 or 24 h, or both incubation periods, expression of all measured genes was dysregulated by the two HDACi, but not by the other mechanistic classes and this difference was highly statistically significant ($P < 0.01$). The exceptions were HCT-116, where there was no significant change in CDKN1A following HDACi treatment although both OVCAR-3 and PC-3 showed greater than 20-fold change in expression of this gene after 24 h belinostat and TSA treatment, but this was not a unique response to HDACi, as other agents also modestly induced CDKN1A; the gene TPX2, encoding a protein that is critical for targeting aurora kinase to the spindle apparatus, was downregulated only in the HCT-116 cell line (approximately five-fold) after 24 h with both belinostat and TSA, but not in the other two cell lines; INCENP, encoding a protein member of the chromosomal passenger complex composed around aurora B kinase, was not significantly changed by treatment with any of the agents.

Evaluation of gene expression changes in xenografts 6 and 24 h after initial treatment with belinostat (200mg/kg, Q1.5 h × 3)

Two xenograft models were chosen to validate the set of selected genes in an in-vivo environment. The A2780 ovarian xenograft was selected to represent a known, sensitive model to this agent [15], although it is not in the NCI-60 panel. The PC-3 xenograft was chosen as a model analogous to the PC-3 cell line used *in vitro*. However, although the two cell lines were similarly sensitive in a clonogenic assay, PC-3 xenografts were not significantly responsive to belinostat when treated under these treatment conditions that rendered the A2780 xenograft sensitive (data not shown). Figure 6a shows a heatmap representation of the belinostat-induced change in expression of the selected set of genes in these in-vivo models. The more sensitive tumor, A2780, has a greater magnitude of change in more genes than the less sensitive xenograft, PC-3. Figure 6b shows a hierarchical clustering, including a relational dendogram, of the best correlated in-vivo and in-vitro samples, reflecting those collected after 6 h *in vivo* and 4 h *in vitro*. Expression profiles from A2780 xenograft samples collected 6 h after the final belinostat dose were well correlated with A2780 xenografts collected after 24 h (PCC = 0.61, $P < 0.001$) and with the PC-3 xenograft samples collected after 6 h (PCC = 0.55, $P = 0.001$), but poorly correlated with the 24 h collection of PC-3 xenografts (PCC = −0.33), reflecting the lack of expression changes measured 24 h after drug treatment in the PC-3 xenograft samples. The xenograft 6 h data, particularly for the drug-sensitive A2780, was well correlated with all the in-vitro data points for all three cell lines (PCC > 0.73, $P < 0.005$). The PC-3 xenograft data was somewhat less correlated with the in-vitro data (PCC = 0.5–0.7, $P < 0.01$), but reflects the lack of sensitivity and absence of robust expression changes in samples collected after 24 h. Finally, Fig. 6b shows a hierarchical clustering and relational dendogram of the best correlated in-vivo and in-vitro samples, reflecting those collected 6 h after the final treatment *in vivo* and 4 h-treated samples *in vitro*. Thus, a group of genes that seem to be differentially and specifically regulated by HDACi *in vitro*, and belinostat

Fig. 4

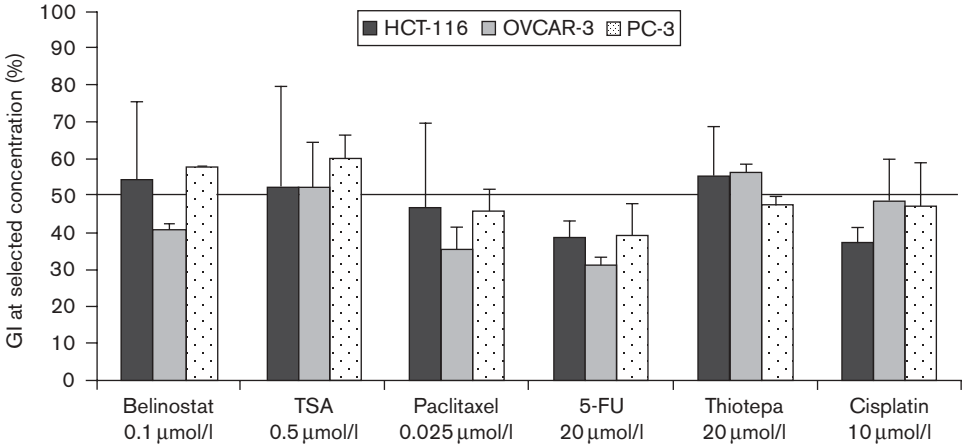

Growth inhibitory (GI) activity of selected concentrations for each selected agent in three cell lines. These growth inhibitory concentrations were calculated from three independent experiments (± SD) after cells were exposed to the drugs for 48 h and surviving cells measured by alamar blue assay.

Fig. 5

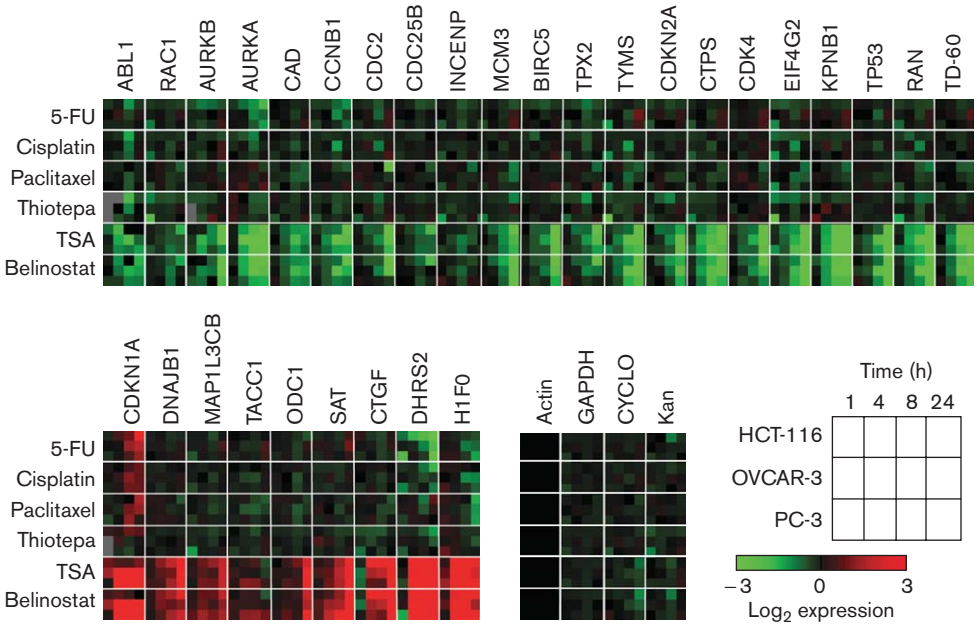

Specificity of histone deactylase inhibitors (HDACi) compared with other antineoplastic agents on a selected set of genes. HCT-116, OVCAR-3, and PC-3 cells were treated at the 50% growth inhibitory concentrations of two HDACi belinostat (0.1 μmol/l) and trichostatin A (TSA) (0.5 μmol/l) along with four mechanistically different antineoplastic agents 5-fluorouracil (5-FU; 20 μmol/l), paclitaxel (0.025 μmol/l), cisplatin (10 μmol/l), and thiotepa (10 μmol/l). Triplicate wells were used for untreated controls and those treated with drugs. Total RNA was isolated 1, 4, 8, and 24 h after drug addition, reversed transcribed, and gene expression measured for 30 test genes, and four control genes utilizing the XP-PCR multiplex assay in three independent experiments. Gene expression changes were calculated (log_2) after normalization to actin and averaged for the triplicate experiments and represented as a heatmap as in Fig. 3. Each block in the heatmap represents the gene expression data for each drug/gene combination where the rows in the blocks are the three cell lines and the columns are the four different times (as outlined in the key). These data indicate that the HDACi response is specific for the majority of genes compared with the other antineoplastic agents.

in vivo, compared with the transcriptional responses for 5-fluorouracil, cisplatin, paclitaxel, and thiotepa (Table 1). Within this group, upregulated genes were CTGF, DHRS2, DNAJB1, H1F0, MAP1LC3B, ODC, SAT, TACC1, and downregulated genes were ABL1, CTPS, EIF4G2, KPNB1, CAD, RAN, TP53, TYMS, and TD-60.

Fig. 6

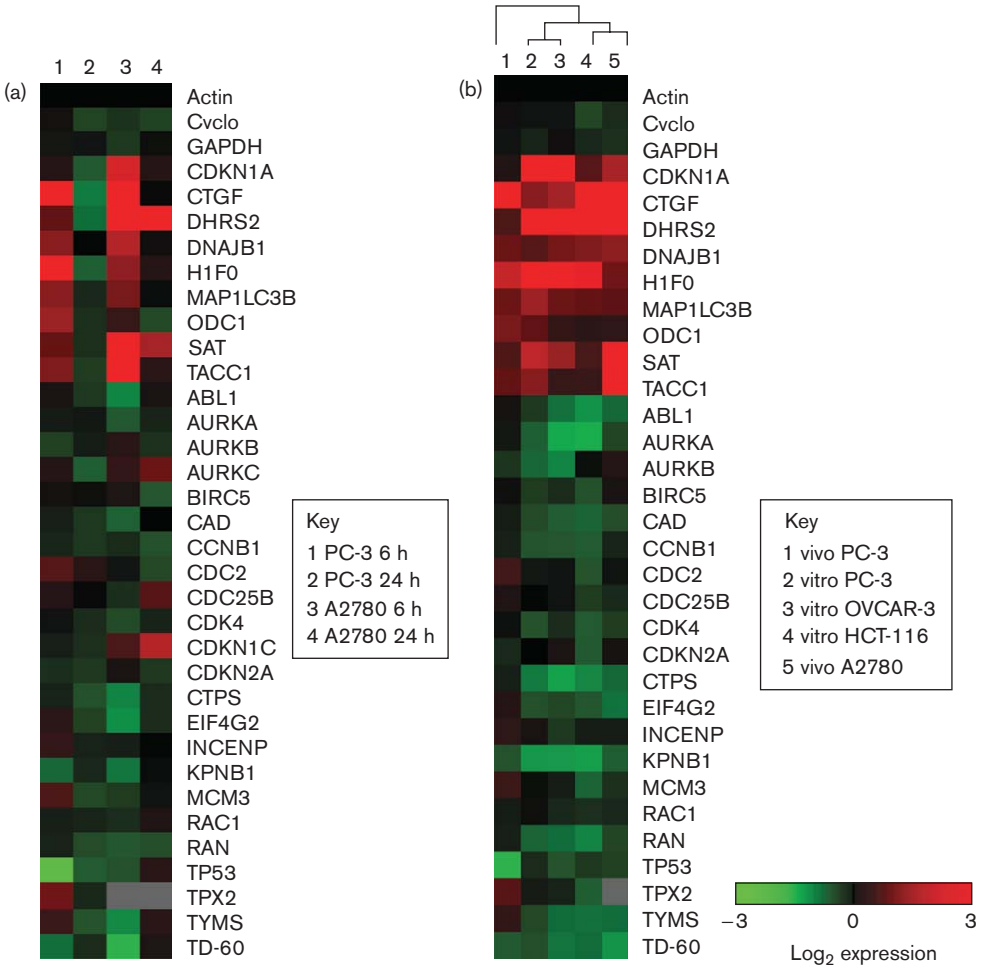

Heatmap representation of genes expression data where red represents upregulated genes and green represents downregulated genes. (a) Heatmap of gene expression levels measured in total RNA isolated from human tumor xenografts (PC-3 and drug-sensitive A2780) collected 6 and 24 h after the final dose from mice treated with belinostat (200 mg/kg Q1.5H × 3). (b) Hierarchical clustering of 6 h xenograft samples and 4 h in-vitro samples (most closely correlated) reflects the similarity of response both *in vitro* and *in vivo*. Xenograft data are averaged from triplicate mice and in-vitro data represent triplicate independent experiments.

Discussion

Results of a phase I study of belinostat indicated this agent was well tolerated, and produced stable disease in 39% of the patients in its first phase I clinical trial [20]. In multiple ongoing phase I and II clinical trials, belinostat has shown promising antitumor activity both as a monotherapy in cutaneous and peripheral T-cell lymphomas, as well as in combination with carboplatin and taxol in solid tumors [30]. The data presented here identifies a drug-induced gene expression signature *in vitro*, which is also reflected in a sensitive xenograft tumor *in vivo*, and seems to be specific to the effects of HDAC inhibition, compared with other mechanisms of antitumor drug action.

Transcription profiling of HCT-116 showed belinostat downregulated genes that regulate mitosis and the cell cycle in general, whereas those involved in chromatin maintenance and nucleosome assembly were upregulated. Moreover, these data included regulation of genes previously reported in response to other HDACi, including cyclins, cyclin-dependent kinases, minichromosome maintenance genes, and members of the redox pathway [9,31]. Twenty-five of the most highly upregulated genes were selected and the cell line cohort was expanded to seven different cell lines. In response to belinostat, these cell lines of different in-vitro sensitivity modulated genes in a similar manner, although with different magnitudes. When the total level of drug-induced gene modulation (i.e. sum of the change of expression of these genes when compared with untreated control) was calculated for all seven cell lines, there was a significant negative correlation ($r = -0.77$, $P = 0.04$) with sensitivity (50% growth inhibitory concentration measured on cell population at

the time of the gene expression studies) (Fig. 4). Thus, the more sensitive the cell line, the greater the magnitude of drug-induced gene expression changes.

These data confirmed a noteworthy reduction of genes involved in the cell cycle, particularly those involved in the G_2/M phase, including genes involved in the aurora kinase pathway, and have shown that belinostat augmented the fraction of cells in the G_2/M phase as was recently shown for PC-3 [32]. Moreover, gene and protein expression of aurora kinase A and B, potentially important chemotherapy targets, were decreased in all cell lines except OVCAR-3. This is in contrast to a recently published report [33] where treatment with hydroxamate-type HDACi in cell lines had no effect on aurora kinase B expression, but in accord with a report in lung cancer cells where both aurora A and B are transcriptionally regulated [29]. We have determined that belinostat does not directly inhibit the kinase activity of either aurora A or aurora B, but does inhibit expression of both these proteins, with modest transcriptional changes in these genes, and other aurora pathway factors (RAN and TD60) [27,28], including inhibitors of cell cycle progression. Many of these cell cycle factors were significantly modulated in the two xenograft models, although under the conditions of treatment we did not observe a notable change (> 1.3-fold) in the gene expression of aurora A or B, indicating that an evaluation of the protein expression would be required to determine whether this target plays an important role in belinostat toxicity *in vivo*.

To determine whether there was a distinctive transcriptional response for belinostat as compared with other chemotherapeutic agents, three cell lines were treated with belinostat, TSA (hydroxamic acid HDACi), 5-fluorouracil, cisplatin, paclitaxel, and thiotepa at equipotent concentrations resulting in 50% growth inhibition. Using a group of 30 genes that included some of the most strongly modulated in the arrays and confirmed by multiplexed reverse transcriptase-PCR (XP-PCR, Beckman Coulter Inc.), and genes known to be involved in regulation of the cell cycle and reported to be altered by HDACi, drug-induced gene expression changes were compared in three cell lines treated over 24 h. These data, from 7344 PCR reactions (Fig. 5), confirmed that this gene group was specific to HDACi compared with 5-fluorouracil, cisplatin, paclitaxel, and thiotepa at equipotent concentrations. With few exceptions, after 8–24 h, each gene was significantly differentially modulated ($P < 0.01$) by belinostat and TSA compared with the other mechanistic classes. Exceptions included CDKN1A, as several of the other agents also induced this labile stress-inducible gene and TPX2, encoding a protein critical for targeting aurora kinase to the spindle apparatus, was downregulated only in the HCT-116 cell line. Thus, we have demonstrated that this set of genes are specifically regulated under these conditions by HDACi, but not agents belonging to the antimetabolite, tubulin inhibitor, and DNA alkylating/interacting classes.

In addition, many of the genes deregulated by belinostat *in vitro* were also confirmed as perturbed *in vivo*, particularly in a sensitive xenograft (A2780), and to a lesser extent in the more resistant PC-3 xenograft. Hierarchical clustering of in-vivo versus in-vitro data (6 h postfinal dose collection and 4 h continuous exposure, respectively), showed that the most closely associated responses are between the A2780 xenograft and the sensitive HCT-116 cell line *in vitro*, whereas the PC-3 xenograft response is somewhat less related. The notable differences in the response time between in-vitro and in-vivo samples, with xenografts showing a greater magnitude of transcriptional response in the 6 h post-dose rather than the 24 h postdose sample (in-vitro response is observed over 4–24 h), probably reflects the short circulating half life of belinostat (0.3–1.3 h) [20], compared with the in-vitro survival time of the drug. Pharmacokinetic studies on *22* patients receiving the maximum tolerated dose, showed a C_{max} of 32.1 μg/ml (101 μmol/l) with a $T_{1/2}$ of 0.69 h [20]. Based on these data, a plasma concentration of 1.0 μmol/l should be maintained for approximately 7 h after infusion. Thus, the genes seen to be dysregulated with 0.5–1.0 μmol/l belinostat 4–8 h after treatment (Figs 5 and 6) might be expected to be reflected in patients, in the same manner as we have seen in the xenograft models.

The most highly and consistently deregulated genes *in vivo* represent genes that underlie a response that seems to be unique to HDACi, and represent genes that may provide insight into the mechanism of sensitivity to belinostat. This transcriptional response represents events including inhibition of the cells mitotic processes shown by downregulation of TD60, a passenger protein whose reduced expression suppresses spindle assembly and blocks cells in prometaphase and KPNB1 which codes for a member of the importin-β, nuclear transport family and has also been identified as a critical mediator of the role of RAN in regulating mitosis and mitotic spindle assembly. Surprisingly, TACC1, which has been reported to be coordinately regulated with its binding partner aurora A [34], is upregulated both *in vivo* and *in vitro* which is inversely expressed to the downregulated aurora kinases. An increased expression of H1F0, a linker histone variant which is involved in differentiation after H4 acetylation, was observed, as was an increase in DHRS2 (HEP27) which has previously been shown to be highly downregulated gene in an established depsipeptide (HDACi) resistant cell line [35]. Genes coding for the polyamine metabolic enzymes SAT (spermine/spermidine N^1-acetyltransferase) and

ornithine decarboxylase (ODC) were upregulated and the latter has been identified as a putative belinostat biomarker [21], suggesting the possible importance of polyamine biosynthesis in the response to belinostat. Both CTPS (CTP synthetase) and TYMS (thymidylate synthetase) have been identified as targets of HDACi [36], and the downregulation of TYMS has provided the basis for combinations of 5-fluorouracil and belinostat in phase I/II trials.

A significant increase in CDKN1C expression was observed in the A2780 xenograft response, in accord with initial microarray data which may reflect the reexpression of this tumor suppressor, cyclin-dependent kinase inhibitor, as has recently been reported for sodium butyrate [37] providing an epigenetic element in the susceptibility of this tumor to belinostat.

These data provide insight into complex underlying mechanisms that are specific for HDACi and the fact that some of the gene changes are consistent across otherwise heterogeneous tumor cell lines and that they occur not only in cell culture, but also in xenograft models, suggests that they may provide tools for optimizing belinostat dosing, activity, and drug combinations.

Acknowledgements

This project has been funded in whole or in part with federal funds from the National Cancer Institute, National Institutes of Health, under contract N01-CO-12400. The content of this publication does not necessarily reflect the views or policies of the Department of Health and Human Services, nor does mention of trade names, commercial products, or organizations imply endorsement by the US Government. This research was supported by the Developmental Therapeutics Program in the Division of Cancer Treatment and Diagnosis of the National Cancer Institute.

References

1 Grunstein M. Histone acetylation in chromatin structure and transcription. *Nature* 1997; **389**:349–352.
2 Jenuwein T, Allis CD. Translating the histone code. *Science* 2001; **293**:1074–1080.
3 Marks PA, Richon VM, Kelly WK, Chiao JH, Miller T. Histone deacetylase inhibitors: development as cancer therapy. *Novartis Found Symp* 2004; **259**:269–281. Discussion 281–288.
4 Bolden JE, Peart MJ, Johnstone RW. Anticancer activities of histone deacetylase inhibitors. *Nat Rev Drug Discov* 2006; **5**:769–784.
5 Marks PA, Richon VM, Rifkind RA. Histone deacetylase inhibitors: inducers of differentiation or apoptosis of transformed cells. *J Natl Cancer Inst* 2000; **92**:1210–1216.
6 Johnstone RW, Licht JD. Histone deacetylase inhibitors in cancer therapy: is transcription the primary target? *Cancer Cell* 2003; **4**:13–18.
7 Chiba T, Yokosuka O, Fukai K, Kojima H, Tada M, Arai M, *et al.* Cell growth inhibition and gene expression induced by the histone deacetylase inhibitor, trichostatin A, on human hepatoma cells. *Oncology* 2004; **66**:481–491.
8 Richon VM, Sandhoff TW, Rifkind RA, Marks PA. Histone deacetylase inhibitor selectively induces p21WAF1 expression and gene-associated histone acetylation. *Proc Natl Acad Sci U S A* 2000; **97**:10014–10019.
9 Peart MJ, Smyth GK, van Laar RK, Bowtell DD, Richon VM, Marks PA, *et al.* Identification and functional significance of genes regulated by structurally different histone deacetylase inhibitors. *Proc Natl Acad Sci U S A* 2005; **102**:3697–3702.
10 Mork CN, Faller DV, Spanjaard RA. A mechanistic approach to anticancer therapy: targeting the cell cycle with histone deacetylase inhibitors. *Curr Pharm Des* 2005; **11**:1091–1104.
11 Blagosklonny MV, Robey R, Sackett DL, Du L, Traganos F, Darzynkiewicz Z, *et al.* Histone deacetylase inhibitors all induce p21 but differentially cause tubulin acetylation, mitotic arrest, and cytotoxicity. *Mol Cancer Ther* 2002; **1**:937–941.
12 Lee KW, Kim JH, Park JH, Kim HP, Song SH, Kim SG, *et al.* Antitumor activity of SK-7041, a novel histone deacetylase inhibitor, in human lung and breast cancer cells. *Anticancer Res* 2006; **26**:3429–3438.
13 Glozak MA, Sengupta N, Zhang X, Seto E. Acetylation and deacetylation of non-histone proteins. *Gene* 2005; **363**:15–23.
14 Plumb JA, Finn PW, Williams RJ, Bandara MJ, Romero MR, Watkins CJ, *et al.* Pharmacodynamic response and inhibition of growth of human tumor xenografts by the novel histone deacetylase inhibitor PXD101. *Mol Cancer Ther* 2003; **2**:721–728.
15 Qian X, La Rochelle WJ, Ara G, Wu F, Petersen KD, Thougaard A, *et al.* Activity of PXD101, a histone deacetylase inhibitor, in preclinical ovarian cancer studies. *Mol Cancer Ther* 2006; **5**:2086–2095.
16 Buckley MT, Yoon J, Yee H, Chiriboga L, Liebes L, Ara G, *et al.* The histone deacetylase inhibitor belinostat (PXD101) suppresses bladder cancer cell growth in vitro and in vivo. *J Transl Med* 2007; **5**:49.
17 Beck HC, Nielsen EC, Matthiesen R, Jensen LH, Sehested M, Finn P, *et al.* Quantitative proteomic analysis of post-translational modifications of human histones. *Mol Cell Proteomics* 2006; **5**:1314–1325.
18 Tumber A, Collins LS, Petersen KD, Thougaard A, Christiansen SJ, Dejligbjerg M, *et al.* The histone deacetylase inhibitor PXD101 synergises with 5-fluorouracil to inhibit colon cancer cell growth in vitro and in vivo. *Cancer Chemother Pharmacol* 2007; **60**:275–283.
19 Feng R, Oton A, Mapara MY, Anderson G, Belani C, Lentzsch S. The histone deacetylase inhibitor, PXD101, potentiates bortezomib-induced anti-multiple myeloma effect by induction of oxidative stress and DNA damage. *Br J Haematol* 2007; **139**:385–397.
20 Steele NL, Plumb JA, Vidal L, Tjornelund J, Knoblauch P, Rasmussen A, *et al.* A phase 1 pharmacokinetic and pharmacodynamic study of the histone deacetylase inhibitor belinostat in patients with advanced solid tumors. *Clin Cancer Res* 2008; **14**:804–810.
21 Dejligbjerg M, Grauslund M, Christensen IJ, Tjornelund J, Buhl Jensen P, Sehested M. Identification of predictive biomarkers for the histone deacetylase inhibitor belinostat in a panel of human cancer cell lines. *Cancer Biomark* 2008; **4**:101–109.
22 Marquard L, Petersen KD, Persson M, Hoff KD, Jensen PB, Sehested M. Monitoring the effect of belinostat in solid tumors by H4 acetylation. *APMIS* 2008; **116**:382–392.
23 Tusher VG, Tibshirani R, Chu G. Significance analysis of microarrays applied to the ionizing radiation response. *Proc Natl Acad Sci U S A* 2001; **98**:5116–5121.
24 Tibshirani R, Hastie T, Narasimhan B, Chu G. Diagnosis of multiple cancer types by shrunken centroids of gene expression. *Proc Natl Acad Sci U S A* 2002; **99**:6567–6572.
25 Hosack DA, Dennis G Jr, Sherman BT, Lane HC, Lempicki RA. Identifying biological themes within lists of genes with EASE. *Genome Biol* 2003; **4**:R70.
26 Eisen MB, Spellman PT, Brown PO, Botstein D. Cluster analysis and display of genome-wide expression patterns. *Proc Natl Acad Sci U S A* 1998; **95**:14863–14868.
27 Silverman-Gavrila RV, Wilde A. Ran is required before metaphase for spindle assembly and chromosome alignment and after metaphase for chromosome segregation and spindle midbody organization. *Mol Biol Cell* 2006; **17**:2069–2080.
28 Rosasco-Nitcher SE, Lan W, Khorasanizadeh S, Stukenberg PT. Centromeric Aurora-B activation requires TD-60, microtubules, and substrate priming phosphorylation. *Science* 2008; **319**:469–472.
29 Zhang XH, Rao M, Loprieato JA, Hong JA, Zhao M, Chen GZ, *et al.* Aurora A, Aurora B and survivin are novel targets of transcriptional regulation by histone deacetylase inhibitors in non-small cell lung cancer. *Cancer Biol Ther* 2008; **7**:1388–1397.
30 Gimsing P. Belinostat: a new broad acting antineoplastic histone deacetylase inhibitor. *Expert Opin Investig Drugs* 2009; **18**:501–508.
31 Butler LM, Zhou X, Xu WS, Scher HI, Rifkind RA, Marks PA, *et al.* The histone deacetylase inhibitor SAHA arrests cancer cell growth, up-regulates

thioredoxin-binding protein-2, and down-regulates thioredoxin. *Proc Natl Acad Sci U S A* 2002; **99**:11700–11705.
32 Qian X, Ara G, Mills E, LaRochelle WJ, Lichenstein HS, Jeffers M. Activity of the histone deacetylase inhibitor belinostat (PXD101) in preclinical models of prostate cancer. *Int J Cancer* 2008; **122**:1400–1410.
33 Park JH, Jong HS, Kim SG, Jung Y, Lee KW, Lee JH, *et al*. Inhibitors of histone deacetylases induce tumor-selective cytotoxicity through modulating Aurora-A kinase. *J Mol Med* 2008; **86**:117–128.
34 Ulisse S, Baldini E, Toller M, Delcros JG, Gueho A, Curcio F, *et al*. Transforming acidic coiled-coil 3 and Aurora-A interact in human thyrocytes and their expression is deregulated in thyroid cancer tissues. *Endocr Relat Cancer* 2007; **14**:827–837.
35 Yamada H, Arakawa Y, Saito S, Agawa M, Kano Y, Horiguchi-Yamada J. Depsipeptide-resistant KU812 cells show reversible P-glycoprotein expression, hyper-acetylated histones, and modulated gene expression profile. *Leuk Res* 2006; **30**:723–734.
36 Glaser KB, Staver MJ, Waring JF, Stender J, Ulrich RG, Davidsen SK. Gene expression profiling of multiple histone deacetylase (HDAC) inhibitors: defining a common gene set produced by HDAC inhibition in T24 and MDA carcinoma cell lines. *Mol Cancer Ther* 2003; **2**:151–163.
37 Cucciolla V, Borriello A, Criscuolo M, Sinisi AA, Bencivenga D, Tramontano A, *et al*. Histone deacetylase inhibitors upregulate p57Kip2 level by enhancing its expression through Sp1 transcription factor. *Carcinogenesis* 2008; **29**:560–567.